

# 低温余热蒸汽闪蒸-双工质联合循环发电系统 热力分析

杨新乐<sup>1</sup>, 黄菲菲<sup>1</sup>, 赵阳升<sup>2</sup>, 戴文智<sup>1</sup>

(1. 辽宁工程技术大学 机械工程学院 辽宁 阜新 123000; 2. 太原理工大学 采矿工艺研究所 山西 太原 030024)

**摘要:**为充分回收矿藏热采过程尾端低温蒸汽余热,提出一种适于蒸汽回收的新型闪蒸-双工质联合循环发电系统,以热力学第一、第二定律为基础,建立了该联合循环热力模型,采用R245fa为循环工质,编制计算程序对系统热效率、输出功率及炯效率进行了热力分析,并将其与单纯闪蒸、双工质朗肯循环进行性能对比。结果表明,在热源温度110℃、压力0.14 MPa情况下,净输出功随闪蒸压力、双工质循环蒸发压力的增大均呈先增大后减小的趋势,当闪蒸压力在0.048 33 MPa,低压级双工质循环蒸发压力为0.389 6 MPa时,系统整体及闪蒸-双工质阶段均存在最大功率,分别为6 249.2 kW、429.2 kW;热效率则随闪蒸压力增大先增大后减小,而随双工质压力的增大不断增大。其中双工质循环的热效率均低于联合循环,在多数情况下单纯闪蒸循环的热效率基本等于联合循环的热效率;炯效率变化规律与净输出功变化规律相同。

**关键词:**低温余热蒸汽;联合循环;闪蒸循环;双工质循环;热力分析

中图分类号:TK212 文献标识码:A

## 引言

注蒸汽开采作为矿藏开采中提高矿藏开采量、保证矿藏开采安全、高效的一种有效途径,在开采技术尾端存在大量低品位能源,如何合理充分地回收这些能源是急待解决的问题<sup>[1]</sup>。双工质循环是一种以低温有机物为工质的闭式朗肯循环<sup>[2]</sup>,也称作有机朗肯循环,它作为回收低温热能的有效方法之一,国内外已经进行了大量的理论和实践研究<sup>[3~6]</sup>。在回收中低温热能方面,有机朗肯循环技术成熟,相对朗肯循环优势明显<sup>[7]</sup>。此外,在地热发电上,单纯闪蒸系统也得到了广泛的应用,吴志坚对闪蒸-

双工质循环联合发电进行了初步研究<sup>[8]</sup>。然而针对矿藏热采低温余热蒸汽,有关闪蒸-双工质联合循环研究不多。本研究在前期工作基础上,为最大化回收低温蒸汽余热,提出一种新型双工质-闪蒸-双工质联合循环模型,使换热过程在不同压力下进行,实现温度与压力的良好匹配及热源的梯级利用,为低温余热蒸汽应用双工质循环充分回收利用提供技术途径和理论依据。

## 1 闪蒸-双工质联合循环发电系统

### 1.1 系统组成及热力过程

以低温余热蒸汽为热源的闪蒸-双工质联合循环发电热力系统及热力循环如图1~图3所示。

循环包含闪蒸系统和2个双工质系统,其中闪蒸系统由闪蒸器、凝汽器以及闪蒸压力对应下的汽轮机组成;双工质系统则由预热器、蒸发器、凝汽器、汽轮机、工质泵和冷却水泵等设备组成。联合循环系统的热力过程如图2所示。

双工质阶段分高压级与低压级两部分。高压级双工质系统包括:4-1(在蒸发器中定压吸热)、1-2(在汽轮机中绝热膨胀)、2-3(在冷凝器中定压放热)、3-4(在工质泵中绝热压缩)4个热力过程。低压级双工质系统与高压级双工质系统热力过程相同。其中,矿藏热采尾端余热蒸汽作为高压级双工质阶段的热源,经过闪蒸器流出的饱和水充当低压级双工质阶段的热源。

闪蒸系统的热源是通过高压级蒸发器流出的未饱和水,其热力过程包括:10-5(从高压级蒸发器

收稿日期:2013-05-24; 修订日期:2013-06-22

基金项目:国家自然科学基金重点项目(50534030),国家自然科学基金青年基金项目(51104083)

作者简介:杨新乐(1980-),男,辽宁盘锦人,辽宁工程技术大学副教授,博士。

中流出的热水在闪蒸器中经扩容降压形成蒸汽的过程)、5—6(闪蒸蒸汽在汽轮机中绝热膨胀)、6—7(乏汽在冷凝器中定压放热) 3个热力过程。

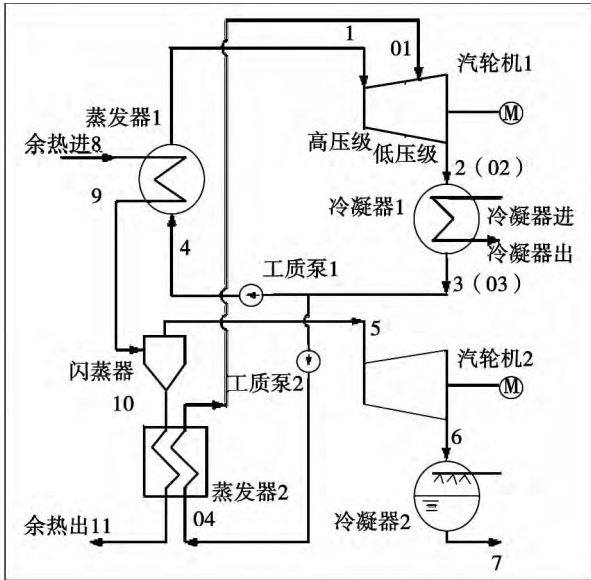


图1 联合循环发电热力系统图

Fig. 1 A diagram of the combined cycle power generation thermal system

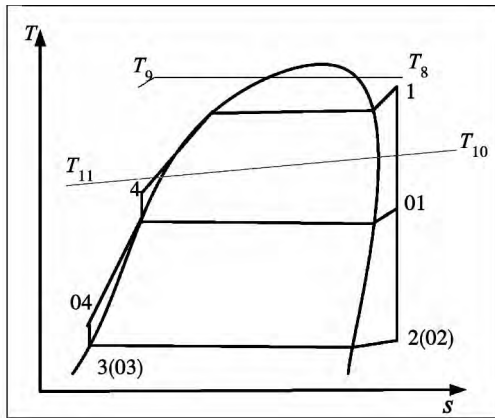


图2 双工质热力循环图

Fig. 2 A diagram of the dual working medium thermal cycle

1.2 系统热力分析理论模型

1.2.1 高压级双工质循环系统

定压加热过程:

$$Q_{e1} = m_g (h_8 - h_9) = m (h_1 - h_4) \quad (1)$$

汽轮机膨胀做功过程:

$$W_{t1} = m (h_1 - h_2) \eta_t \quad (2)$$

定压放热过程:

$$Q_{c1} = m (h_2 - h_3) \quad (3)$$

绝热压缩过程:

$$W_{p1} = m (h_4 - h_3) / \eta_p \quad (4)$$

净功率:

$$P_{net1} = (W_{t1} - W_{p1}) \cdot \eta_m \cdot \eta_e \quad (5)$$

热效率:

$$\eta_1 = P_{net1} / Q_{e1} \quad (6)$$

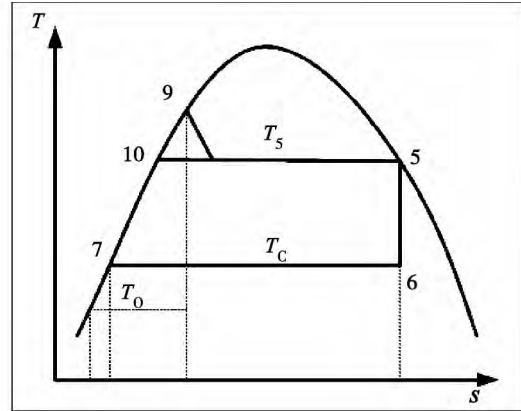


图3 闪蒸系统热力循环图

Fig. 3 A diagram of the thermal cycle of a flash system

1.2.2 闪蒸系统

根据闪蒸器的热平衡得:

$$Q_{e2} = mg (h_9 - h_{10}) = q_{m1} (h_5 - h_{10}) \quad (7)$$

净功率:

$$P_{net2} = q_{m1} (h_5 - h_6) \eta_t \cdot \eta_m \cdot \eta_e \quad (8)$$

热效率:

$$\eta_2 = P_{net2} / Q_{e2} \quad (9)$$

1.2.3 低压级双工质循环系统

定压加热过程:

$$Q_{e3} = q_{m0} (h_{01} - h_{04}) = (m_g - q_{m1}) (h_{10} - h_{11}) \quad (10)$$

汽轮机膨胀做功过程:

$$W_{t3} = q_{m0} (h_{01} - h_{02}) \eta_t \quad (11)$$

定压放热过程:

$$Q_{c3} = q_{m0} (h_{02} - h_{03}) \quad (12)$$

绝热压缩过程:

$$W_{p3} = q_{m0} (h_{04} - h_{03}) / \eta_p \quad (13)$$

净功率:

$$P_{net3} = (W_{t3} - W_{p3}) \eta_m \cdot \eta_e \quad (14)$$

热效率:

$$\eta_3 = P_{net3} / Q_{e3} \quad (15)$$

1.2.4 整体联合循环系统

系统总功率:

$$P_{net} = P_{net1} + P_{net2} + P_{net3} \quad (16)$$

系统热效率:

$$\eta = \frac{P_{net}}{Q} = \frac{P_{net1} + P_{net2} + P_{net3}}{Q_{e1} + Q_{e2} + Q_{e3}}$$

$$= \frac{P_{net1} + P_{net2} + P_{net3}}{Q_{e1} + Q_{e2} + q_{m0}(h_{01} - h_{04})} \quad (17)$$

系统焓效率:

$$E_h = m_g [(h_8 - h_0) - T_0(s_8 - s_0)] \quad (18)$$

$$\eta_{ex} = \frac{P_{net}}{E_h} = \frac{P_{net1} + P_{net2} + P_{net3}}{m_g [(h_8 - h_0) - T_0(s_8 - s_0)]} \quad (19)$$

式中:  $m_g$ —热源质量流量, kg/s;  $m$ 、 $q_{m1}$ 、 $q_{m0}$ —工质质量流量, kg/s;  $h$ —比焓, kJ/kg;  $W$ —功率, kW;  $Q$ —热流量, kJ/s;  $s$ —比熵, kJ/(kg · K);  $\eta$ —热效率;  $\eta_{ex}$ —焓效率;  $P$ —净功率, kW;  $E_h$ —输入焓, kJ/s;  $T$ —温度, K; 角标  $t$ 、 $m$ 、 $g$ —汽轮机内效率、机械效率及发电机效率;  $e$ —蒸发器;  $c$ —冷凝器;  $p$ —工质泵;  $t$ —汽轮机;  $1 \sim 11$ —工质和热源各状态点;  $0$ —环境;  $net$ —净值。

## 2 系统热力计算结果及分析

以对流热采油页岩过程低温余热蒸汽为研究对象, 余热源初始状态为 110 °C、0.14 MPa 的饱和蒸汽, 单井筒流量 100 t/h, 设定经过高压级双工质循环阶段热源出口温度为 109 °C, 压力为 0.14 MPa, 将剩余具有一定显热的水通过闪蒸-双工质联合循环系统与有机工质进行换热, 带动发电机发电, 计算过程中取  $\eta_t = 0.65$ ,  $\eta_p = 0.8$ ,  $\eta_m = 0.85$ ,  $\eta_e = 0.85$  根据文献 [1 ~ 2, 9] 的推荐, 选取 R245fa 作为循环工质, 其中双工质阶段背压取 0.2 MPa, 闪蒸系统中冷凝温度设定为 30 °C。

### 2.1 系统热力性能与 $p_{sz}$ 、 $p_{01}$ 的关系

#### 2.1.1 $P_{net}$ 与 $p_{sz}$ 、 $p_{01}$ 的关系

图 4 所示为闪蒸阶段净输出功率  $P_{net2}$  与闪蒸压力  $p_{sz}$  的关系。从图中可以看出随着闪蒸压力  $p_{sz}$  的增大  $P_{net2}$  先增大然后逐渐减小。随着闪蒸压力的增加, 一方面通过闪蒸得到的蒸汽在汽轮机中的焓降由于压降的增加而逐渐增大, 另一方面由于在较大压力下饱和蒸汽的比焓较大, 在进入闪蒸器热源温度、流量一定时, 闪蒸得到的蒸汽流量随压力增大会逐渐降低。因此在该阶段净输出功率会存在一个最大值, 出现先增大后减小的趋势。

图 5 表示低压级双工质阶段净输出功率  $P_{net3}$  在不

同闪蒸压力下随该阶段蒸发压力  $p_{01}$  的变化规律。由于净输出功率  $P_{net3}$  是进入汽轮机中蒸汽流量与单位质量蒸汽在汽轮机中焓降的函数, 所以其变化规律类似闪蒸阶段。同时, 随闪蒸压力增大, 进入低压级双工质循环阶段的热源水流量及其饱和水焓值升高, 蒸发器中有机工质流量相应增大, 因此随闪蒸压力  $p_{sz}$  的增加, 低压双工质循环阶段净输出功率不断增大, 且最大净输出功率对应的蒸发压力  $p_{01max}$  也不断提高, 而当  $p_{sz}$  很小时  $p_{01max}$  也很小, 因此在闪蒸压力为 0.019 44 MPa 时, 只出现随  $p_{01}$  增加  $P_{net3}$  减小的部分。

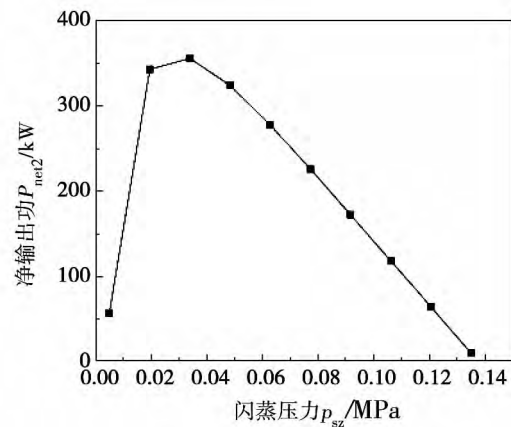


图 4 不同闪蒸压力下闪蒸阶段净输出功率的变化规律

Fig. 4 Variation law governing the net output power in the flash stage under various flash pressures

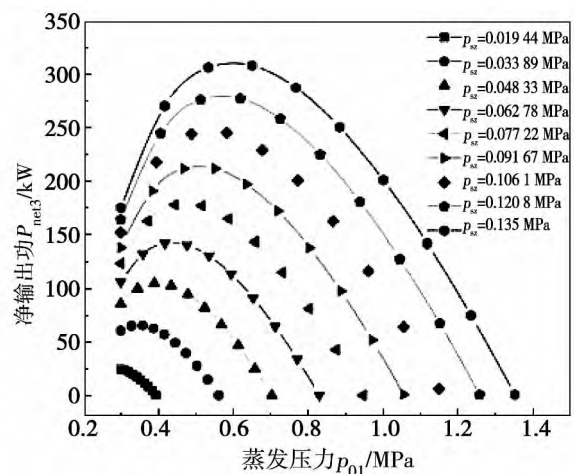


图 5 低压双工质阶段净输出功率随蒸发压力的变化规律

Fig. 5 Variation law governing the net output power in the stage of low pressure dual working medium operation with the evaporation pressure

图 6 表示在整个系统中净输出功率  $P_{net}$  随闪蒸压力及双工质阶段蒸发压力的变化。由于在高压级双工质循环阶段取热源出口温度  $T_9 = 109\text{ }^\circ\text{C}$  ,蒸发压力  $p_1 = 1.4\text{ MPa}$  时,  $P_{net1} = 5\ 820\text{ kW}$  为定值。而  $P_{net2}$  随闪蒸压力  $p_{sz}$  的先增大后减小,  $P_{net3}$  随  $p_{sz}$  的增加而增加, 整个系统的净输出功率是 3 个阶段净输出功率之和, 即  $P_{net} = P_{net1} + P_{net2} + P_{net3}$ 。因此  $P_{net}$  随闪蒸压力  $p_{sz}$  的增长会呈现出先增大后减小的趋势, 且增大的幅度逐渐减小; 在闪蒸压力一定时, 闪蒸系统净输出功率  $P_{net2}$  也是确定的,  $P_{net}$  随  $p_{01}$  的变化规律只与  $P_{net3}$  有关, 其变化规律与  $P_{net3}$  相同, 呈先增大后减小的趋势。在  $p_{sz} = 0.048\ 33\text{ MPa}$  ,  $p_{01} = 0.389\ 6\text{ MPa}$  时, 系统存在最大净输出功率  $P_{net} = 6\ 249.2\text{ kW}$ 。

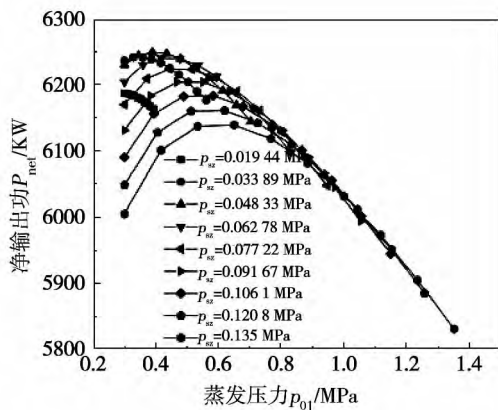


图 6 系统净输出功率随蒸发压力的变化规律  
Fig. 6 Variation law governing the net output power of the system with the evaporation pressure

2.1.2 系统热效率  $\eta$  与  $p_{sz}$ 、 $p_{01}$  的关系

根据式 (9)  $\eta_2$  只与闪蒸压力有关, 闪蒸压力增加, 闪蒸汽轮机焓降增大, 因此热效率逐渐增大, 但随着闪蒸压力的升高, 闪蒸器出口饱和蒸汽焓降也在升高, 所以热效率又会出现增幅逐渐减小的趋势, 如图 7 所示。在汽轮机效率为定值的理论情况下, 双工质阶段效率  $\eta_3$  同样也只与蒸发压力有关, 当  $p_{01}$  增大,  $\eta_3$  也随之增大如图 8 所示。

如图 9 所示, 对于整体系统, 热效率  $\eta$  为整个系统中的净输出功率与吸收热量的比值。高压级双工质循环阶段有机工质在换热器中吸收的热量  $q_1$  是确定的; 在闪蒸阶段, 随闪蒸压力的增大, 在闪蒸器中通过降压得到的蒸汽流量会减小, 而单位蒸汽汽化潜热也会变小, 因此该阶段吸热量  $q_2$  随  $p_{sz}$  的增

加逐渐减少; 在低压级双工质循环阶段, 系统吸热量  $q_3$  随闪蒸压力的升高而增加, 随  $p_{01}$  的增大而减小, 这是由于  $p_{01}$  增大时, 热源出蒸发器的温度会提高, 进而在蒸发器中吸热量会减少。这样由于低压双工质阶段吸热量增大幅度大于闪蒸阶段吸热量减小幅度, 整个系统吸热量随闪蒸压力  $p_{sz}$  增大而增大。所以在  $p_{01}$  相同时,  $\eta$  随  $p_{sz}$  先增大后减小; 在闪蒸压力一定时,  $\eta$  随  $p_{01}$  的增加而逐渐增加, 增加的幅度逐渐变缓。

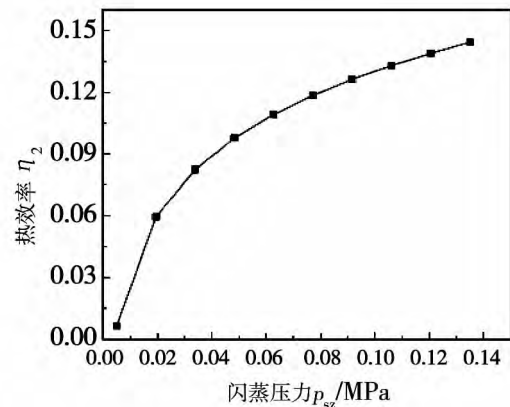


图 7 闪蒸阶段热效率随闪蒸压力的变化规律  
Fig. 7 Variation law governing the thermal efficiency in the flash stage with the flash pressure

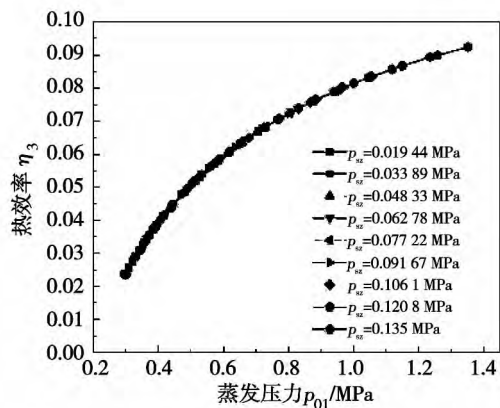


图 8 低压双工质阶段热效率随蒸发压力的变化规律

Fig. 8 Variation law governing the thermal efficiency in the stage of low pressure dual working medium operation with the evaporation pressure

2.1.3 焓效率  $\eta_{ex}$  与  $p_{sz}$ 、 $p_{01}$  的关系

在热力发电系统中, 蒸发器、凝汽器和汽轮机都

存在较大的焓损失,其中由于换热温差的存在,蒸发器焓损失最大。随着双工质阶段蒸发压力的增大,工质与热源换热温差减小,吸热过程中熵增减小,焓损失减少,但随蒸发压力增大热源工质出口温度会增大,直接排向环境未经利用的热源焓增多,在闪蒸器中亦是如此。因此如图 10 所示,焓效率变化规律与  $P_{net}$  随  $p_{sz}$ 、 $p_{01}$  的变化规律相同,在闪蒸压力  $p_{sz} = 0.04833 \text{ MPa}$ 、 $p_{01} = 0.3896 \text{ MPa}$  时,焓效率取得最大值为  $\eta_{ex} = 0.4196$ 。

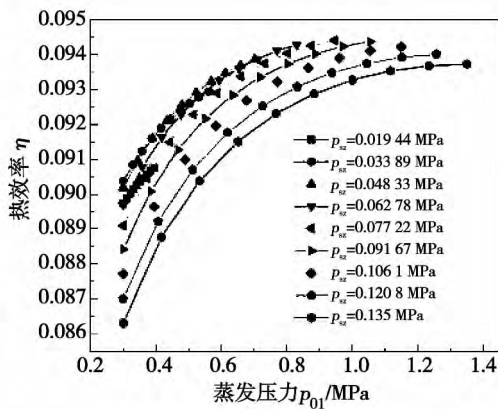


图 9 系统热效率随低压级蒸发压力的变化规律  
Fig. 9 Variation law governing the thermal efficiency of the system with the evaporation pressure of the low pressure stage

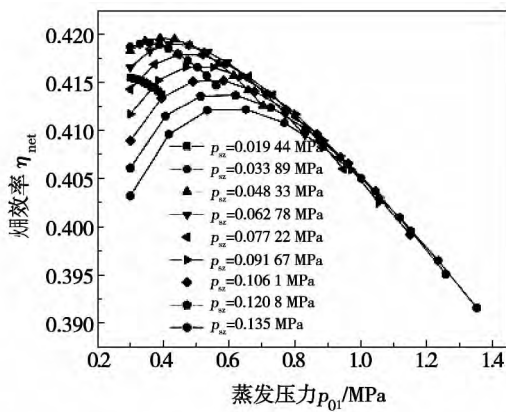


图 10 系统焓效率随低压级蒸发压力的变化规律  
Fig. 10 Variation law governing the exergy efficiency of the system with the evaporation pressure of the low pressure stage

## 2.2 不同循环系统热力性能比较

### 2.2.1 净输出功率 $P_{net}$ 比较

以高压级双工质循环系统出来的  $109 \text{ }^\circ\text{C}$ 、 $0.14$

MPa 热水为热源,通过闪蒸-双工质系统联合做功与相同热源情况下单纯闪蒸系统、单纯双工质系统的净输出功率进行比较。由图 11 可以看出在允许范围内,任意闪蒸压力下联合循环阶段净输出功率都高于其相应蒸发压力下单纯双工质系统的净输出功率;当闪蒸压力小于  $0.1206 \text{ MPa}$  时,联合循环阶段的净输出功率也将高于单纯闪蒸系统最大净输出功率。通过计算得知,单纯闪蒸系统中最大净输出功率为  $355.9 \text{ kW}$ ,单纯双工质系统的最大净输出功率为  $314.7 \text{ kW}$ ,而闪蒸-双工质联合系统的最大净输出功率为  $429.2 \text{ kW}$ ,比相同热源情况下闪蒸系统和双工质系统分别提高了  $17\%$ 、 $26.7\%$ 。

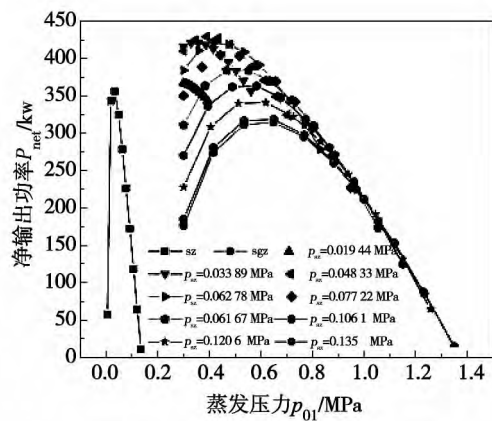


图 11 不同系统净输出功率随蒸发压力的变化规律

Fig. 11 Variation law governing the net output power of the system with the evaporation pressure

### 2.2.2 系统热效率比较

如图 12 所示,单纯闪蒸系统热效率随闪蒸压力增加不断增加,在闪蒸压力  $p_{sz} = 0.135 \text{ MPa}$  时热效率取得最大值  $14.42\%$ ;单纯双工质系统随蒸发压力增加也呈逐渐增加的趋势,但增加的幅度减缓,当双工质压力大于  $1.0 \text{ MPa}$  时,热效率几乎不变,在蒸发压力为  $1.375 \text{ MPa}$  时,效率达到最大值为  $9.246\%$ ;对于闪蒸-双工质联合系统,随  $p_{sz}$  的增大  $\eta$  先增大后减小,随双工质阶段蒸发压力的变化则呈递增关系,开始增加逐渐减缓,在大于一定蒸发压力后,增幅逐渐增大。通过计算可以得到在不同闪蒸压力下,单纯闪蒸系统的热效率与联合系统的最大热效率基本接近,而单纯双工质系统的热效率则普遍低于对应联合系统的热效率。

设高压级净输出功率为定值,由于闪蒸-双工质

联合系统具有更高的做功能力 较高的热效率,所以可以认为双工质-闪蒸-双工质联合循环的性能优于双工质-闪蒸系统,优于压力级不同的双工质-双工质系统。在工程实际中,为了更好的利用低品位热源,针对低温余热蒸汽可以考虑利用双工质-闪蒸-双工质联合循环系统,但同时也增加了闪蒸器和闪蒸汽轮机的成本。在技术经济可行的条件下,还可以考虑采取不同的有机工质,以吸收不同温度范围内的热量,更好的实现能量的梯级利用。

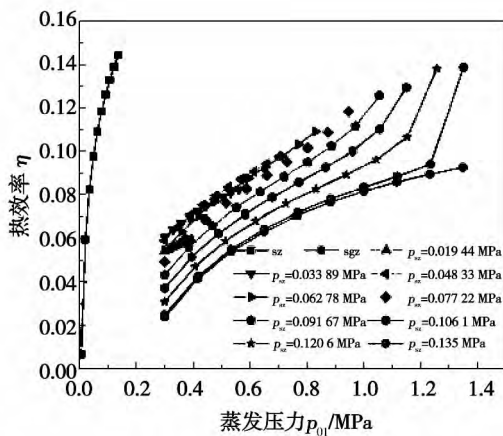


图 12 不同系统热效率随蒸发压力的变化规律  
Fig. 12 Law governing a change of the efficiency of different system under the different evaporating pressures

### 3 结 论

(1) 在相同热源情况下,闪蒸-双工质联合系统的净输出功随  $p_{sz}$ 、蒸发压力  $p_{01}$  的增大均呈先增大后减小的趋势,相较于单纯闪蒸系统或双工质系统其净输出功分别提高约 17%、26.7% 左右;

(2) 闪蒸-双工质联合系统的热效率  $\eta$  随闪蒸压力的增大先增大后减小,随低压级蒸发压力的增加逐渐增加,但增幅先减缓再升高;与单纯闪蒸系统相比,两者的热效率相近;双工质系统的热效率明显低于联合系统;

(3) 与单纯闪蒸系统、双工质系统相比,联合系统由于具有较大净输出功,热效率与闪蒸系统相近,而双工质系统热效率、净输出功最小,因此联合系统性能优于单纯闪蒸、双工质系统。

### 参考文献:

[1] 杨新乐,赵阳升,冯增朝. 对流热采油页岩过程低温余热 ORC 系统热力分析[J]. 热能动力工程 2012 27(6): 664-669.  
YANG Xin-le, ZHAO Yang-sheng, FENG Zeng-chao. Thermodynamic analysis of a low temperature waste heat organic rankine cycle system in the process of the convection heat-based oil shale exploitation[J]. Journal of Engineering for Thermal Energy. 2012 27(6): 664-669.

[2] Bahaa Saleh, Gerald Koglbauer, Martin Wendland. Working fluids for low-temperature organic rankine cycles[J]. Energy, 2005, 32(7): 1210-1221.

[3] Hung T C. Waste heat recovery of organic rankine cycle using dry fluids[J]. Energy Conversion and Management 2001 42(5): 539-553.

[4] Philippe Roy, Martin Desilets, Nicolas Galanis. Thermodynamic analysis of a power cycle using a low-temperature source and a binary  $NH_3-H_2O$  mixture as working fluid[J]. International Journal of Thermal Sciences. 2009 49: 48-58.

[5] Galanis N, Cayer E, Roy P. Electricity generation from low temperature sources[J]. Journal of Applied Fluid Mechanics. 2009, 2(2): 55-67.

[6] Hettiarachchi H D, Golubovic M, Worek, Ikegami Y. Optimum design criteria for an organic rankine cycle using low-temperature geothermal heat sources[J]. Journal of Energy Resources Technology 2007 129(3): 24-37.

[7] 江 龙, Eicichard A. Groll. 有机朗肯循环的发电系统的实验研究[J]. 制冷学报 2012 33(1): 18-21.  
JIANG Long, Eicichard A. Groll. Experimental study of an organic rankine cycle power generation system[J]. Journal of Refrigeration 2009 30(3): 316-321.

[8] 吴志坚, 龚宇烈, 马伟斌. 闪蒸-双工质循环联合地热发电系统研究[J]. 太阳能学报 2009 30(3): 316-321.  
WU Zhi-jian, GONG Yu-lie, MA Wei-bin. Research of a flash-dual working medium combined cycle geothermal power generation system[J]. Acta Energetica Solaris Sinica 2009 30(3): 316-321.

[9] 刘 杰, 陈江平, 祁照岗. 低温有机朗肯循环的热力学分析[J]. 化工学报 2010 61(S2): 9-14.  
LIU Jie, CHEN Jiang-ping, QI Zhao-gang. Thermodynamic analysis of a low temperature organic Rankine cycle[J]. Journal of Chemical Industry 2010 61(S2): 9-14.

(丛 敏 编辑)

燃气轮机燃烧室点火位置及点火过程计算 = **Calculation of the Ignition Location and Process for the Combustor of a Gas Turbine** [刊 汉] ZHENG Hong-tao ,LI Ya-jun ( College of Energy and Power Engineering ,Harbin Engineering University ,Harbin ,China ,Post Code: 150078) ,LI Ya-jun ( Department of Gas Turbine Cause ,CSIC Harbin No. 703 Research Institute ,Harbin ,China ,Post Code: 150078) ,CAI Lin ( Department of Power and Energy Source ,CSIC Wuhan No. 701 Research Institute ,Wuhan ,China ,Post Code: 430064) //Journal of Engineering for Thermal Energy & Power. -2014 29( 1) . -22 ~ 28

By using the software Fluent ,the authors studied the ignition location and flame propagation process in the combustor of a gas turbine with the optimum ignition location ,turbulent flow flame propagation speed and flame propagation characteristics of the combustor being obtained. It has been found that it is capable of finding out the optimum ignition location inside the combustor by using the method gradually shortening the flame core radius. At the optimum ignition location ,there exists a secondary return flow zone and its presence ensures a successful ignition while the main flow return zone plays a role of stabilizing the flame. The secondary and main flow return zones play an irreplaceable role in the ignition process of the combustor. The vaporization of the oil drops leads to a delay of the ignition and the turbulent flow flame propagation speed is around 6.5 m/s. **Key words:** gas turbine ,combustor ,ignition location ,ignition process ,numerical simulation

低温余热蒸汽闪蒸-双工质联合循环发电系统热力分析 = **Thermodynamic Analysis of a Low Temperature Waste Heat Steam Flash Vaporization-Dual Working Medium Combined Cycle Power Generation System** [刊 汉] YANG Xin-le ,HUANG Fei-fei ,DAI Wen-zhi ( College of Mechanical Engineering ,Liaoning University of Engineering Technology ,Fuxin ,China ,Post Code: 123000) ZHAO Yang-sheng ( Mining Process Research Institute ,Taiyuan University of Science and Technology ,Taiyuan ,China ,Post Code: 030024) //Journal of Engineering for Thermal Energy & Power. -2014 29( 1) . -29 ~ 34

To fully recover the low temperature steam waste heat in the tail portion of hot production processes of various mine deposits ,proposed was a new type flash vaporization-dual working medium combined cycle power generation system. On the basis of the first and second law of the thermodynamics ,a model for such a system was established with R245fa serving as the working medium of the cycle and a program was prepared and designed to perform a thermodynamic analysis of the thermal efficiency ,output power and exergy efficiency of the system and a comparison of the performance between a simple flash vaporization and dual working medium Rankine cycle. It has been found that under the condition of the heat source attaining a temperature of 110 °C and a pressure of 0.14 MPa ,the net output power of the system will assume a tendency of first increase and then decrease with an increase of the flash vaporization pressure and the vaporization pressure of the dual working medium cycle. When the flash vaporization pressure stands at 0.04833 MPa and the vaporization pressure of the low pressure stage dual working medium cycle vaporiza-

tion pressure hits 0.3896 MPa, the system as a whole and the flash vaporization-dual working medium section will all have their maximum output power, being 6249.2 and 429.2 kW respectively. The thermal efficiency will first increase and then decrease with an increase of the flash vaporization pressure but continuously grow with a rise of the pressure of the dual working medium. Among them, the thermal efficiency of the dual working medium cycle is invariably lower than that of the combined cycle. In the most cases, that of the single flash vaporization cycle is basically equal to that of the combined cycle while the law governing the variation of the exergy efficiency is identical to that governing the variation of the net output power. **Key words:** low temperature waste heat steam, combined cycle, flash cycle, dual working medium cycle, thermodynamic analysis

1350 MW 二次再热发电机组热力系统设计分析 = **Analysis of the Design of a Thermal System for a 1350 MW Secondary Reheat Power Generator Unit** [刊, 汉] YAN Wei-ping, ZHAO Yong-ming, LI Hai-xin (College of Energy Source, Power and Mechanical Engineering, North China University of Electric Power, Baoding, China, Post Code: 071003), LIU Li-heng (Guodian Science and Technology Research Institute, Nanjing, China, Post Code: 210000) // Journal of Engineering for Thermal Energy & Power. -2014, 29(1). -35~40

With the design coordination between both sides of the boiler and steam turbine being taken into account in a comprehensive way, set up was a 1350 MW secondary reheat unit principle thermal system. For different configurations of the feedwater pump steam turbines, a calculation and analysis were performed with the influence of two versions of feedwater pump-purposed steam turbines on the reheat steam flow rate, heat rate of the unit and design of the reheater etc. being quantitatively analyzed, namely, back pressure and extraction type and condensing type steam turbine. It has been found that under the rated load operating condition, the steam flow rates of the primary and secondary reheater of the back pressure and extraction type feedwater pump steam turbine thermal system are 266 and 289 t/h smaller than those of the condensing type one, thus making for the design of the convection heating surface of the boiler. Compared with the steam inlet temperatures of No. 4 and 5 heaters in the condensing type steam turbine system, those of the back pressure and extraction type steam turbine thermal system will lower by 350 and 297 °C respectively, favorable for the design and operation of the heaters. However, the heat rate of the back pressure and extraction type steam turbine thermal system version is 6 kJ/kW·h higher than that of the condensing type steam turbine thermal system version. Under the partial load operating conditions, the calculation results show that the primary and secondary reheat steam flow rates of the back pressure and extraction type steam turbine thermal system is still lower than those of the condensing type steam turbine thermal system and the heat rate of the former is still a bit excessively high. **Key words:** secondary reheat, thermal system, design of the convection heating surface in a boiler, feedwater pump-purposed steam turbine

ORC 系统热力性能计算程序编写 = **Development of a Program for Calculating the Thermal Performance of**